# 5

# Microwave Transmission Lines

This chapter describes the characteristics of several transmission lines commonly used at microwave frequencies. For efficient transmission, coaxial lines and rectangular waveguides are usually employed.[1] Low-loss coax is used mostly at frequencies below 5 GHz, while rectangular guide is the popular choice at the higher frequencies. Circular waveguides find application where the capability of transmitting or receiving waves having more than one plane of polarization is required. Circular guides employing the $TE_{01}$ mode are also useful for ultra low-loss transmission at high microwave frequencies.

Small sections of transmission lines are often utilized as circuit elements at microwave frequencies. Their use as inductors, capacitors, resonant circuits, and transformers has been described in Chapters 3 and 4. For these applications, strip-type transmission lines, coaxial lines, waveguide sections, and occasionally a short length of open two-wire line are employed.

## 5–1 THE OPEN TWO-WIRE LINE

The transmission of electrical energy with open two-wire lines is usually restricted to frequencies below 500 MHz. One of its most familiar forms is the TV twin-lead used to connect an antenna to a television set. The reason it is not used at higher frequencies is due to its tendency to radiate energy at a discontinuity or bend in the line. This radiation represents a loss in transmitted power, which generally is unacceptable. However, since small lengths are occasionally used as circuit elements, its characteristics are summarized here.

[1] The efficiency of transmission lines and antenna systems is compared in Appendix F.

The electric and magnetic field pattern for the open two-wire line is shown in Fig. 5–1. In most cases, the spacing between the wires $s$ is much greater than their radius $a$. Typically, $s$ is greater than $4a$. For the electric and magnetic fields shown, power flow ($\vec{\mathbf{E}} \times \vec{\mathbf{H}}$) is into the page. Since both electric and magnetic fields are transverse to the direction of propagation, this represents a *TEM mode*. Other modes of propagation are possible in which portions of the electric and magnetic field are longitudinally oriented. These modes can be suppressed by choosing $s \ll \lambda$.

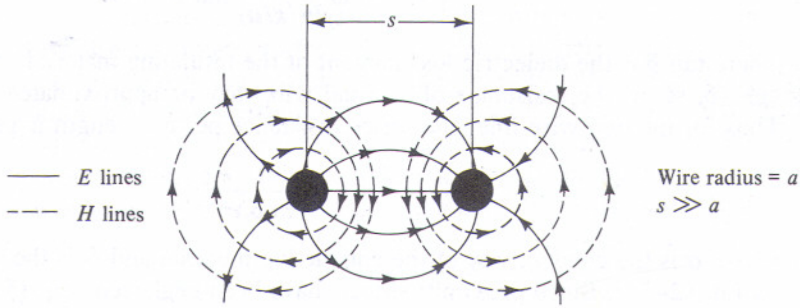


**Figure 5–1** The electromagnetic field pattern for TEM transmission on an open two-wire line.

For the TEM mode, the inductance and capacitance per unit length are given by the following approximate expressions. For $s < 4a$,

$$L' \approx \frac{\mu_0 \mu_R}{\pi} \ln \frac{s}{a} \qquad \text{and} \qquad C' \approx \frac{\pi \epsilon_0 \epsilon_R}{\ln (s/a)} \tag{5–1}$$

These represent the high-frequency values, since it has been assumed that the skin depth $\delta_s \ll a$. This means that most of the ac currents are located near the surface of the conductors. The derivation of these expressions is given in Chapter 6 of Ref. 5–1. For high-frequency, low-loss lines, the characteristic impedance $Z_0$ is given by Eq. (3–21). Substituting in the above expressions yields

$$Z_0 \approx 120 \sqrt{\frac{\mu_R}{\epsilon_R}} \ln \frac{s}{a} = 276 \sqrt{\frac{\mu_R}{\epsilon_R}} \log \frac{s}{a} \qquad \text{ohms} \tag{5–2}$$

since $\mu_0 = 4\pi \times 10^{-7}\ H/m$ and $\epsilon_0 = 8.854 \times 10^{-12}\ F/m$. When rigid conductors are used, the dielectric medium surrounding the conductors is usually air and hence $\mu_R$ and $\epsilon_R$ are unity.

An expression for the velocity of propagation can be obtained by substituting Eq. (5–1) into Eq. (3–24). The result is

$$v = \frac{1}{\sqrt{\mu_0 \mu_R \epsilon_0 \epsilon_R}} = \frac{c}{\sqrt{\mu_R \epsilon_R}} \tag{5–3}$$

which is exactly Eq. (2–53), namely, the wave velocity in an unbounded dielectric medium. This same result holds for the coaxial line in the TEM mode [Eq. (3–27)]. In fact, this conclusion can be generalized to any transmission line operating in the

TEM mode. Assuming a uniform dielectric material occupies all the insulating region between the two conductors, wave velocity, wavelength, and phase constant are given by Eqs. (2–53), (2–55), and (2–56), respectively.

Approximate expressions for the shunt conductance and series resistance per unit length of the open two-wire line are given below. With $G' = \omega C' \tan \delta$ [(see Eq. (2–23)], the shunt conductance per unit length is

$$G' \approx \omega \frac{\pi \epsilon_0 \epsilon_R}{\ln (s/a)} \tan \delta \tag{5-4}$$

where $\tan \delta$ is the dielectric loss tangent of the insulating material. At high frequencies ($\delta_s \ll a$), the resistance of a round wire may be approximated by Eq. (2–79). Thus for the two-wire line, the series resistance per unit length is given by

$$R' \approx \frac{1}{\pi a \delta_s \sigma} \tag{5-5}$$

where $\sigma$ is the conductivity of the conducting material and $\delta_s$ is the skin depth given by Eq. (2–73). Since proximity effects have been neglected, Eq. (5–5) is only valid for $s > 4a$. Using the above expressions, the attenuation constant may be determined from Eq. (3–22). Attenuation versus frequency curves for high-frequency lines are available from the various cable manufacturers. Data sheets also provide the *velocity factor* for each line, where

$$\text{Velocity Factor} \equiv \frac{v}{c} = \frac{\lambda}{\lambda_0} \tag{5-6}$$

and $v$ is the wave velocity for the particular transmission line. If the conductors are completely immersed in a nonmagnetic insulator of dielectric constant $\epsilon_R$, the velocity factor is equal to $1/\sqrt{\epsilon_R}$. In many cases, however, the insulating region contains two or more dielectric materials. Two examples are shown in Fig. 5–2. Part *a* shows the familiar TV twin-lead, where the two wires are separated by a thin piece of foam rubber, while part *b* shows a coaxial line with a loose-fitting teflon sleeve. In both examples, the velocity factor lies somewhere between $1/\sqrt{\epsilon_R}$ and unity (that is, $v = c$). For instance, the velocity factor for the TV twin-lead is practically unity (typically > 0.90) since most of the insulating region is air. On the other hand, for

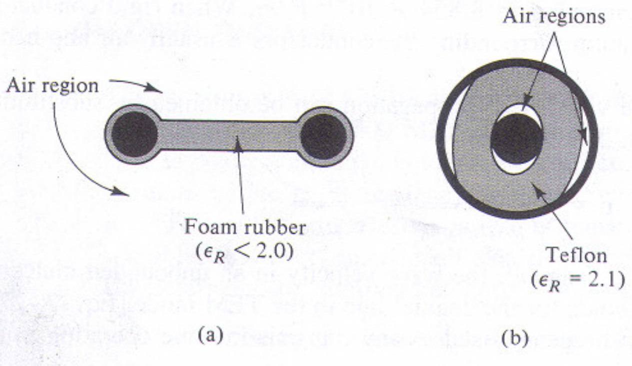


**Figure 5–2** Examples of transmission lines with a nonuniform insulating region.

the coaxial line shown in part $b$, a major portion of the insulating region is teflon ($\epsilon_R = 2.1$) and hence the velocity factor is slightly greater than $1/\sqrt{2.1} = 0.69$.

## 5–2 THE COAXIAL LINE

Unlike the open two-wire line, the coaxial line is nonradiating since the electric and magnetic fields are confined to the region between the concentric conductors. For this reason, it is widely used as a high-frequency transmission line. Before 1960, most applications were confined to frequencies below 3.0 GHz. With the advent of precision connectors and miniaturized lines, they are now used extensively in low power applications at $X$ and $K_u$ band and in some cases as high as $K_a$ band.[2]

The TEM mode pattern for the coaxial line was described earlier (Fig. 3–8). The high-frequency inductance and capacitance are given by Eqs. (2–31) and (2–21). These expressions may be rewritten on a per unit length basis. Namely,

$$L' = \frac{\mu_0 \mu_R}{2\pi} \ln \frac{b}{a} \qquad \text{and} \qquad C' = \frac{2\pi \epsilon_0 \epsilon_R}{\ln (b/a)} \tag{5–7}$$

where the conductor radii $a$ and $b$ are defined in Fig. 3–8. Equations for $v$, $\lambda$, and $\beta$ are given by Eqs. (3–27), (3–28), and (3–29), respectively. The high-frequency characteristic impedance of the coaxial line is given by Eq. (3–30) and repeated here.

$$Z_0 = 60 \sqrt{\frac{\mu_R}{\epsilon_R}} \ln \frac{b}{a} = 138 \sqrt{\frac{\mu_R}{\epsilon_R}} \log \frac{b}{a} \qquad \text{ohms} \tag{5–8}$$

The shunt conductance per unit length may be obtained from Eq. (2–23).

$$G' = \omega \frac{2\pi \epsilon_0 \epsilon_R}{\ln (b/a)} \tan \delta \tag{5–9}$$

The series resistance per unit length is the sum of the resistances due to the inner and outer conductors. Since at high frequencies $\delta_s \ll a$,

$$R' \approx \frac{1}{2\pi a \delta_s \sigma} + \frac{1}{2\pi b \delta_s \sigma} = \frac{a + b}{2\pi a b \delta_s \sigma} \tag{5–10}$$

The attenuation per unit length for a low-loss line is given by Eq. (3–22). Namely,

$$\alpha \approx \frac{R'}{2Z_0} + \frac{G' Z_0}{2} = \alpha_c + \alpha_d$$

where $\alpha_c$ and $\alpha_d$ represent the portions due to the imperfect conductors and insulator, respectively. Making use of Eq. (5–8), one can derive the following expressions for $\alpha_c$ and $\alpha_d$ (Prob. 5–5).

$$\alpha_c = 13.6 \frac{\delta_s \sqrt{\epsilon_R} \{1 + (b/a)\}}{\lambda_0 b \ln (b/a)} \qquad \text{dB/length} \tag{5–11}$$

[2] The more common microwave bands are listed in Table 1–1.

and

$$\alpha_d = 27.3 \frac{\sqrt{\epsilon_R}}{\lambda_0} \tan\delta \qquad \text{dB/length} \tag{5-12}$$

where $\delta_s$ is the skin depth in the metal conductors and $\tan\delta$ is the dielectric loss tangent of the insulator. These equations are valid only if both conductors and the dielectric are nonmagnetic, which is usually the case. Values of loss tangent at 3 GHz for several dielectrics are listed in Appendix B.

An excellent source of microwave data is the Microwave Engineers' Handbook (Ref. 5–4). The section on coaxial lines contains graphs of attenuation and power capacity versus frequency for a variety of rigid and flexible cables.

**Voltage breakdown in coaxial lines.** The electric field at any point between the concentric conductors of a coaxial line is given by Eq. (3–26) and is repeated here.

$$E = \frac{V}{r \ln(b/a)} \tag{5-13}$$

where $r$ is the radius to the particular point between the conductors ($a \le r \le b$) and $E$ and $V$ represent rms values of the ac quantities. Since the largest value of electric field occurs at $r = a$, voltage breakdown of the dielectric occurs initially near the surface of the inner conductor. To avoid this condition, its peak value ($\sqrt{2}E$) at $r = a$ must be less than the dielectric strength of the insulator ($E_d$). Thus the maximum allowable rms voltage across the coaxial line is given by

$$V_{\max} = \frac{a E_d}{\sqrt{2}} \ln\frac{b}{a} = \frac{b E_d}{\sqrt{2}} \frac{\ln(b/a)}{(b/a)} \tag{5-14}$$

At room temperature and a pressure of one atmosphere, $E_d \approx 3 \times 10^6$ V/m for air. Therefore, for an air-insulated line with, say $b = 2$ cm and $a = 1$ cm, the applied voltage must be less than 14,700 V rms. Since standing waves are possible along the line, the maximum allowable voltage may be considerably less, namely, $V_{\max}/(1 + |\Gamma_L|)$.

The maximum power that can be transmitted along a match terminated coaxial line without causing voltage breakdown in the insulator is

$$P_{\max} = \frac{V_{\max}^2}{Z_0} = \frac{(bE_d)^2}{120}\left(\frac{a}{b}\right)^2 \sqrt{\frac{\epsilon_R}{\mu_R}} \ln\frac{b}{a} \qquad \text{watts} \tag{5-15}$$

where $Z_0$ is given by Eq. (5–8) and $V_{\max}$ by Eq. (5–14). If $Z_L \neq Z_0$, standing waves exist along the line. For large standing waves ($|\Gamma_L| \approx 1$), the actual power handling capability is one-fourth that given by this equation since the electric field at a voltage maximum is approximately twice that associated with the incident wave. In practice, an additional safety factor is usually included to account for surface roughness and other mechanical imperfections.[3]

[3] Since most good insulators have a higher dielectric strength ($E_d$) than air, it seems that higher power capability could be achieved with dielectric-filled lines. However, if the dielectric is not a perfect mechanical fit (see Fig. 5–2b), the opposite can occur! The reason is that the electric field in the air gaps can actually be greater than when the line is completely air-filled.

Since arcing is an extremely fast process, even short pulses of microwave power must be kept below this limit. Thus Eq. (5–15) represents a *peak power* limitation for the coaxial line. Its *average* power capacity is usually limited by heating effects due to the dissipation associated with $\alpha_c$ and $\alpha_d$.

Before describing how the voltage and power handling capability of the coaxial line can be optimized by the proper choice of dimensions, a discussion of higher-order modes is necessary.

**Higher-mode propagation in coaxial lines.** The principal mode of propagation in a coaxial line is the TEM mode. Its field pattern is shown in Fig. 3–8. Most coaxial components (detectors, attenuators, filters, etc.) are designed on the basis that the input signal will be in the TEM mode. There are, however, other ways in which electromagnetic energy can propagate along a coaxial line. These are called higher-order propagation modes. These higher modes can only propagate when the signal frequency exceeds a certain value. This value is known as the cutoff frequency of the mode and is denoted by $f_c$. At frequencies below $f_c$, the signal decays exponentially with distance as it attempts to propagate along the line.[4] The field patterns and cutoff frequencies of these modes can be obtained by solving Maxwell's equations and applying the boundary conditions associated with the coaxial structure. The solutions, found in Sec. 8.10 of Ref. 5–6, are beyond the scope of this discussion. However, an approximate expression for the cutoff of the $TE_{11}$ mode in a coaxial line may be deduced by analogy with rectangular waveguide propagation. This argument is presented by Wheeler (Sec. 5.1 of Ref. 5–2). The following expressions for cutoff wavelength ($\lambda_c$) and frequency are accurate to within 5 percent for $b/a < 7$.

$$\lambda_c \approx \pi(a+b) \qquad \text{and} \qquad f_c = \frac{v}{\lambda_c} \approx \frac{c}{\pi(a+b)\sqrt{\mu_R \epsilon_R}} \tag{5–16}$$

The $TE_{11}$ mode is especially important since its cutoff frequency is the lowest of all the higher-order modes. A sketch of its field pattern is shown in Fig. 5–3.

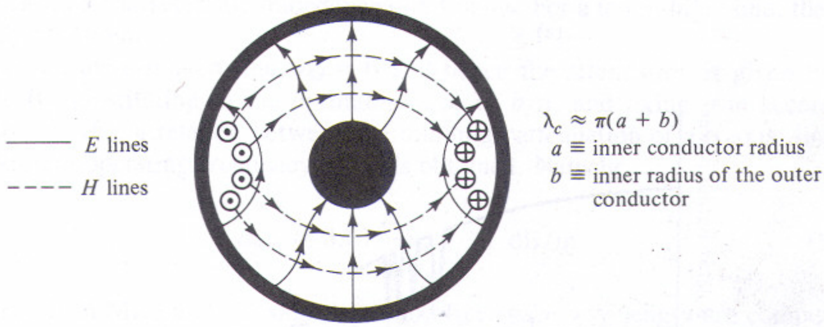


**Figure 5–3** The electromagnetic field pattern for the $TE_{11}$ mode in a coaxial line.

[4] When $f < f_c$, the higher-order mode is said to be *evanescent* since its exponential decay with distance from the exciting source is associated with energy storage rather than dissipation.

In coaxial transmission, one usually desires TEM mode propagation without the presence of higher-order modes. The reason can be understood with the aid of Fig. 5–4. Part *a* of the figure shows a fixed-power, variable-frequency generator, a coaxial line, and a power meter. Part *b* shows a typical curve of output power versus frequency. As the generator frequency is increased, the power output decreases gradually due to skin effect and dielectric loss [Eqs. (5–11) and (5–12)]. Increasing the frequency further, however, leads to sudden decreases in output power over narrow frequency bands as indicated in the figure. These *resonant-like* losses are associated with higher-mode propagation in the coaxial line, particularly the $TE_{11}$ mode. When the signal enters the coaxial line, some of it is converted from the TEM to the $TE_{11}$ mode. At frequencies greater than the cutoff frequency of the $TE_{11}$ mode, this power propagates to the output. Since the power meter has been designed to accept TEM signals, most of the $TE_{11}$ mode is reflected back toward the input where it is partially re-reflected. For certain values of electrical length ($\beta l$), the resultant multiple reflections create a resonance condition with its accompanying high loss. This was explained in Sec. 3–2. To avoid this condition, use of the coaxial line should be restricted to frequencies *below* the cutoff frequency of the $TE_{11}$ mode. Denoting the maximum operating frequency as $f_{max}$ and using Eq. (5–16) yields

$$f_{max} < f_c = \frac{c}{\pi(a+b)\sqrt{\mu_R \epsilon_R}} \tag{5–17}$$

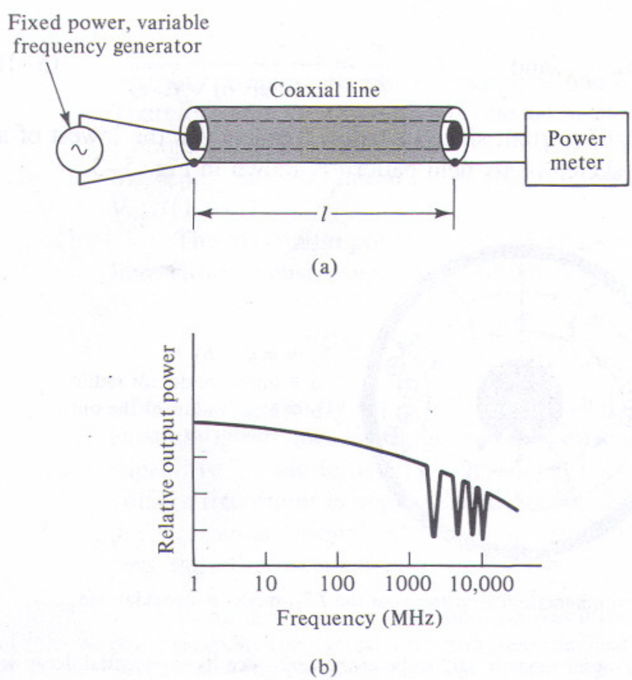


**Figure 5–4** The effect of higher-mode propagation on power transmission.

In designing a coaxial line, it is customary to allow a 5 percent safety factor. As a result, $f_{max}$ is usually defined as 0.95 $f_c$. Thus, for a given $a/b$ ratio, the *maximum* allowable value of $b$ that insures single-mode (TEM) propagation for all frequencies up to $f_{max}$ is

$$b_{max} = \frac{0.95c}{\pi f_{max}\left(1 + \frac{a}{b}\right)\sqrt{\mu_R \epsilon_R}} \tag{5–18}$$

Many coaxial components (for example, filters and transformers) utilize the radius of the inner conductor $a$ as a design variable. To insure against $TE_{11}$ mode propagation for any and all values of $a$, the worst case is assumed (namely, $a/b \approx 1$), which leads to the following conservative value for $b_{max}$.

$$b_{max} = \frac{0.95c}{2\pi f_{max}\sqrt{\mu_R \epsilon_R}} \tag{5–19}$$

Note that in either case, the higher the required frequency range, the smaller the value of $b_{max}$ and hence for a fixed $b/a$ ratio, the lower the power-handling capability of the line [Eq. (5–15)]. Thus a compromise is usually required between high power and high operating frequency. This *design tradeoff* occurs quite often in electrical engineering work.

**Optimizing transmission characteristics in coaxial lines.** The $b/a$ ratio of a coaxial line and hence its characteristic impedance can be chosen to minimize attenuation, maximize voltage breakdown, or maximize power handling capability. All three cases are considered here.

***1. $Z_0$ for minimum attenuation.*** Since $\alpha_d$ is not a function of dimensions, the attenuation constant $\alpha$ is minimized when $b/a$ is chosen to minimize $\alpha_c$. For a given value of $f_{max}$, $b_{max}$ is given by Eq. (5–18). By substituting $b_{max}$ into Eq. (5–11), differentiating the result with respect to $b/a$ and setting it equal to zero yields $b/a = 4.68$ as the optimum value. When the line is air-insulated, this is equivalent to a characteristic impedance of 93 ohms. For a teflon-filled line, the optimum $Z_0$ is 64 ohms.

For an air-insulated line, $\alpha_d = 0$ and hence the attenuation is given by Eq. (5–11). By substituting in the optimum value of $b/a$, and fixing $b$ in accordance with Eq. (5–18), a relation between the minimum attenuation of a coaxial line and its maximum operating frequency ($f_{max}$) is obtained. Namely,

$$\alpha_{min} = 0.67\frac{\delta_s}{\lambda_0}f_{max} \qquad \text{dB/m} \tag{5–20}$$

where $f_{max}$ is in MHz and the skin depth and free space wavelength are computed at the frequency of interest. For example, suppose the required value of $f_{max}$ is 12,000 MHz. Then for minimum attenuation, $b/a = 4.68$ and from Eq. (5–18) $b$ is set equal to 0.623 cm. For copper conductors, $\delta_s$ is given by Eq. (2–75). Substituting into Eq. (5–20) yields an attenuation of 0.10 dB/m at 3 GHz and 0.18 dB/m at 10

GHz. In practice, surface roughness and other factors cause the actual attenuation to be slightly greater than the calculated value. It is important to note that lowering $f_{max}$ allows the use of larger conductors [Eq. (5–18)] which reduces the attenuation.

***2. $Z_0$ for maximum voltage breakdown.*** The transmission of high voltage pulses along a coaxial line usually requires that the line be optimized for maximum voltage breakdown. For a given value of $f_{max}$, the optimum $b/a$ ratio is 3.59, which is equivalent to a 77 ohm, air-insulated line. This result is obtained by substituting $b_{max}$ into Eq. (5–14), differentiating with respect to $b/a$ and setting the result equal to zero.

***3. $Z_0$ for maximum power handling capacity.*** Assuming that the maximum power that a coaxial line can handle is limited by the dielectric strength of the insulator, one would think that the optimum $b/a$ ratio would be the same as in the previous case. However, this is not so since $P = V^2/Z_0$ and $Z_0$ is also a function of the $b/a$ ratio. For a given value of $f_{max}$, the optimum $b/a$ ratio is 2.09. This means that for an air-insulated line, the optimum $Z_0$ for maximum power handling capacity is 44 ohms. This result is obtained by substituting $b_{max}$ into Eq. (5–15), differentiating with respect to $b/a$ and setting the result equal to zero.

A relationship between power capacity and maximum operating frequency can be obtained by substituting the optimum value of $b/a$ into Eq. (5–15) and setting $b$ in accordance with Eq. (5–18). The result for an air-insulated coaxial line is

$$P_{max} = 5.3\left(\frac{E_d}{f_{max}}\right)^2 \quad \text{watts} \tag{5–21}$$

where $f_{max}$ is in MHz and $E_d$ in V/m. For example, if $f_{max} = 14{,}000$ MHz and $E_d = 3 \times 10^6$ V/m, $P_{max} = 243$ kW. Allowing for the possibility of high standing waves along the line, this value should be reduced by a factor of four. Therefore, the maximum power that can be safely transmitted along an air-insulated coaxial line with a maximum usable frequency of 14 GHz is about 60 kilowatts. This value can be increased somewhat by pressurizing the air in the coaxial line. For example, at a pressure of two atmospheres, the value of $E_d$ is 50 percent greater than its value under normal atmospheric conditions.

Although the characteristic impedances obtained in the three cases discussed here are optimum for a fixed value of $f_{max}$, the fact of the matter is that moderate deviations from these values have only a small effect on the parameter being optimized (see Probs. 5–9 and 5–10). Furthermore, it is important as a practical matter to standardize on a value of $Z_0$. This is especially true in the manufacture and use of connectors, measurement equipment, and standard components. Except for the occasional use of 75 ohm line, coaxial lines and equipment are usually designed for $Z_0 = 50$ ohms. This represents a satisfactory compromise, as explained in Sec. 5.7 of Ref. 5–2.

## 5–3 STRIP-TYPE TRANSMISSION LINES

Strip-type transmission lines are used in the design and construction of complex microwave systems and components. Generally, the line consists of either one or two copper-clad, dielectric sheets with the desired circuit etched on one side. Its main advantage lies in the fact that the photo-etching technique used in its manufacture is both accurate and economical. A photograph of a stripline filter is shown in Fig. 5–5. Transitions between coaxial and strip transmission are shown at either end of the filter. Strip configurations may be either symmetrical or asymmetrical. In this text, the symmetrical type is called *stripline* while the asymmetric arrangement is denoted as *microstrip*. Before discussing their characteristics, formulas will be presented for the case of parallel-plate transmission (Fig. 5–6). Although seldom used as a transmission line, its characteristics are sometimes utilized in analyzing other microwave lines. For this reason, a brief summary is presented.

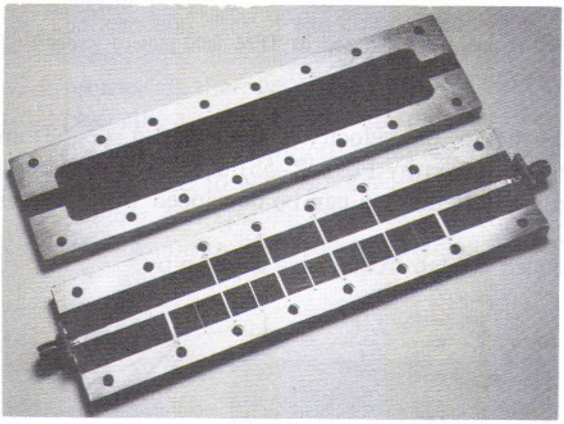

**Figure 5–5** A stripline microwave filter. (Courtesy of M/A-COM, Inc., Burlington, Mass.)

**Parallel-plate transmission.** A cross-sectional view of the parallel-plate transmission line is pictured in Fig. 5–6. It consists of a low-loss dielectric sandwiched between two flat metal conductors. Usually, its width is much greater than the conductor spacing ($w \gg b$) and the metal thickness is quite small ($t \ll b$). Therefore, it is assumed that the only significant fields lie in the dielectric region between the conductors and that they are uniform. A sketch of the electric and magnetic fields is shown in the figure. Since, at high frequencies, the skin depth in the conductor is small compared to its thickness, most of the current and charge reside on the inner conductor surfaces (that is, the ones in contact with the dielectric). For these conditions, the resistance and capacitance per unit length are given by

$$R' = \frac{2}{w\delta_s \sigma} \tag{5–22}$$

and

$$C' = \frac{w}{b}\epsilon_0 \epsilon_R \tag{5–23}$$

The first equation represents the resistance per length of the two conductors and follows directly from the conclusion below Eq. (2–77). Equation (5–23) derives directly from the parallel-plate capacitance formula, Eq. (2–19), where the area $A$ is the product of the conductor length and its width. For $w \gg b$, the assumption that all the electromagnetic energy is confined to the uniform dielectric region ($\epsilon_R$) is

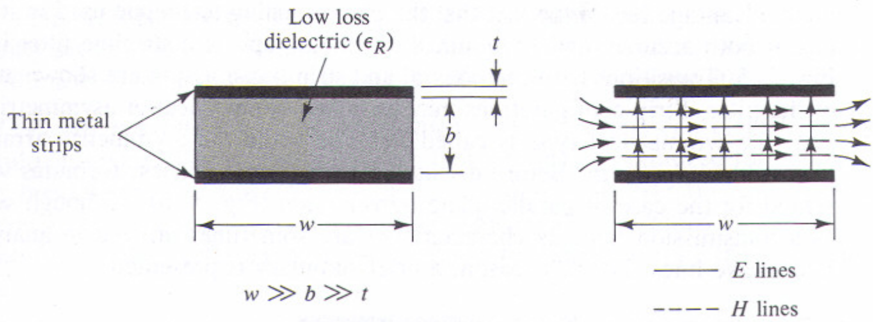


**Figure 5–6** A parallel-plate transmission line and its TEM field pattern (cross-sectional view).

valid. Thus for the TEM mode shown, the velocity is given by Eq. (2–53) and the wavelength and phase constant are given by Eqs. (2–55) and (2–56), respectively. As a result, expressions for $Z_0$ and attenuation can be developed without having to derive equations for $L'$ and $G'$.

The characteristic impedance at high frequencies is given by

$$Z_0 \approx \sqrt{\frac{L'}{C'}} = \frac{\sqrt{L'C'}}{C'} = \frac{1}{vC'}$$

With $v = c/\sqrt{\mu_R \epsilon_R}$,

$$Z_0 \approx 377\frac{b}{w}\sqrt{\frac{\mu_R}{\epsilon_R}} \qquad \text{ohms} \tag{5–24}$$

As before, the attenuation constant is given by $\alpha_c + \alpha_d$, where for low-loss lines, $\alpha_c = R'/2Z_0$ and $\alpha_d = G'Z_0/2$. Making use of Eqs. (5–22), (5–24), and (2–73) and the equality 1 Np = 8.686 dB results in the following expression.

$$\alpha_c = 27.3\frac{\delta_s\sqrt{\epsilon_R}}{b\lambda_0} \qquad \text{dB/length} \tag{5–25}$$

This equation assumes nonmagnetic conductors and dielectric. Since $\lambda_0 \propto 1/f$ and $\delta_s \propto 1/\sqrt{f}$, the attenuation due to the conductors is proportional to $\sqrt{f}$.

The attenuation per unit length due to the dielectric is given by

$$\alpha_d = \frac{G'Z_0}{2} = \frac{\omega C'}{2}Z_0 \tan\delta = \pi f\sqrt{L'C'}\tan\delta$$

where use has been made of Eq. (2–22). With $\sqrt{L'C'} = 1/v$ and $v = f\lambda$,

$$\alpha_d = \frac{\pi}{\lambda}\tan\delta = \frac{\pi}{\lambda_0}\sqrt{\epsilon_R}\tan\delta \qquad \text{Np/length}$$

or

$$\alpha_d = 27.3\,\frac{\sqrt{\epsilon_R}}{\lambda_0}\tan\delta \qquad \text{dB/length} \tag{5–26}$$

where again a nonmagnetic dielectric has been assumed. Note that this equation is identical to $\alpha_d$ for a coaxial line [Eq. (5–12)]. In both cases, $\alpha_d$ is directly proportional to frequency since $\lambda_0$ is inversely proportional to $f$.

**Symmetrical strip transmission (stripline).** For the past 25 years, most strip-transmission systems have made use of the symmetrical configuration, usually called *stripline*. Two of the best sources for information on stripline techniques are Harlan Howe's book (Ref. 5–3) and the IEEE Transactions on Microwave Theory and Techniques (Ref. 5–13). Figure 5–7 shows a cross-sectional view of the stripline structure and its TEM mode pattern. Note the similarity between its mode pattern and that of the coaxial line (Fig. 3–8). With voltage applied between the center strip and the pair of ground planes, current flows down the center strip and returns via the two ground planes. Although the structure is open at the sides, it is basically a nonradiating transmission line. In practice, however, any unbalance in the line causes energy to be radiated out the sides. To prevent this, the ground planes are shorted to each other with either screws or rivets as shown in the figure. The number and spacing of the shorting screws are adjusted to prevent higher-mode propagation in the frequency range of interest.

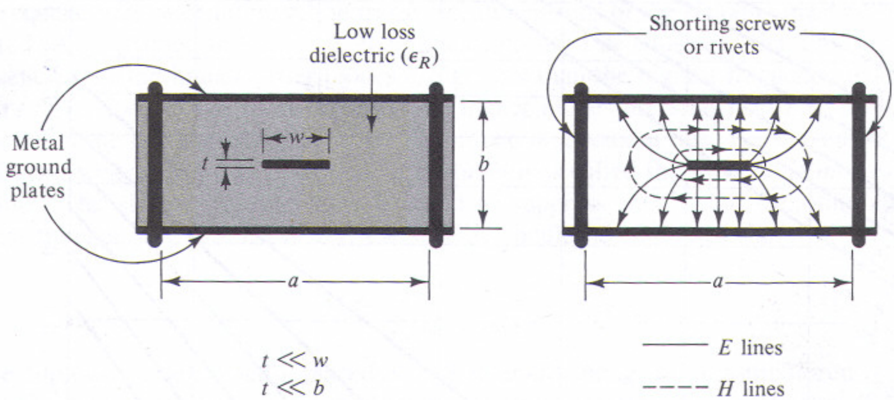


**Figure 5–7** A symmetrical strip transmission line (stripline) and its TEM field pattern (cross-sectional view).

With all the fields confined to the uniform dielectric ($\epsilon_R$), the velocity, wavelength, and phase constant for the TEM mode are given by Eqs. (2–53), (2–55), and (2–56). The characteristic impedance may be derived from the expression above Eq. (5–24). Namely,

$$Z_0 = \frac{1}{vC'} = \frac{\sqrt{\mu_R \epsilon_R}}{3 \times 10^8 C'} \qquad \text{ohms} \tag{5–27}$$

Thus the determination of the high-frequency characteristic impedance reduces to finding the capacitance per unit length of the stripline configuration. A variety of approximate solutions are available in the literature. The one obtained by Cohn (Ref. 5–14) is probably the most widely used. The results are shown graphically in Fig. 5–8. Since the stripline is usually constructed using a pair of printed circuit boards, the thickness $t$ is typically a few thousandths of an inch, while $b$ ranges from 1/16 to

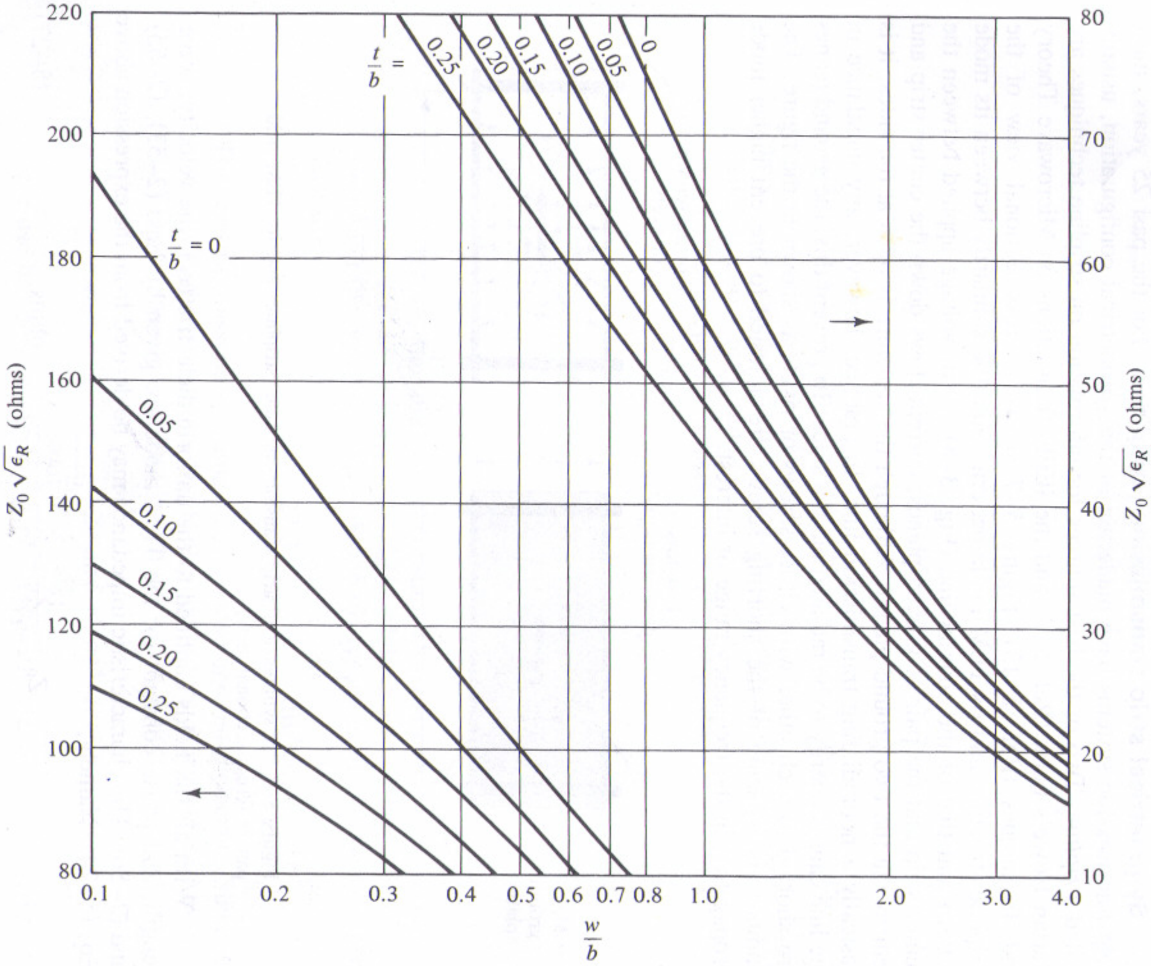


**Figure 5–8** Characteristic impedance data for stripline. A nonmagnetic dielectric is assumed ($\mu_R = 1.0$). Also $a \gg w$ and $a > 2b$. (From S. Cohn, Ref. 5–14; © 1955 IRE now IEEE, with permission.)

1/4 of an inch. For this configuration, practical values of $Z_0$ range from about 10 to 100 ohms for most dielectrics. A discussion of the dielectric materials normally used in stripline is given in Chapter 1 of Ref. 5–3.

The stripline attenuation due to the dielectric material ($\alpha_d$) is the same as for coaxial and parallel-plate transmission [Eq.(5–26)]. The attenuation associated with the conductors has been derived by Cohn (Ref. 5–14) and others. Normalized values ($\overline{\alpha}_c$) for copper striplines are given in Fig. 5–9. Using the value of $\overline{\alpha}_c$ from the graph, $\alpha_c$ is obtained from the following equation,

$$\alpha_c = \overline{\alpha}_c \frac{\sqrt{f \epsilon_R}}{b} \qquad \text{dB/length} \tag{5–28}$$

where the frequency $f$ is in GHz and $b$ is the ground-plate spacing. As before, the attenuation for low-loss lines is the sum of $\alpha_c$ and $\alpha_d$.

The stripline configuration is basically a low-power transmission system. Typically, it is used at power levels of less than 100 W, average, and 1000 W, peak. A more complete discussion of its power capability is given in Chapter 1 of Ref. 5–3.

As with other transmission lines, stripline is capable of propagating electromagnetic energy in other modes. In order to insure only TEM mode propagation in the frequency range of interest, the transverse dimensions of the stripline must be restricted. As explained in Sec. 5–2, the dimensions must be chosen so that the cutoff frequencies for the higher-order modes are greater than the highest frequency of interest ($f_{\max}$). Two of the more troublesome higher modes are shown in Fig. 5–10. The one on the left is analogous to the $TE_{11}$ mode in a coaxial line. For reasons that will become clear in the next section, it is sometimes called the *waveguide mode* in stripline. The shorting screws may be used to suppress this mode. Denoting the highest frequency of interest is $f_{\max}$, the spacing should be chosen so that

$$a < \frac{c}{2 f_{\max} \sqrt{\mu_R \epsilon_R}} \tag{5–29}$$

These suppressors are usually placed at $\lambda/8$ intervals along the transmission direction, where $\lambda$ is calculated at the highest frequency of interest. The mode shown on the right in Fig. 5–10 does not occur as often as the *waveguide* mode. It can be suppressed by adjusting the ground-plane spacing so that

$$b < \frac{c}{4 f_{\max} \sqrt{\mu_R \epsilon_R}} \tag{5–30}$$

**Asymmetric strip transmission (microstrip).** With the advent of low-loss, high dielectric constant materials, microstrip has become increasingly popular, particularly in the fabrication of microwave integrated circuits (see Sec. 6–7). The line consists of a thin conductor and a ground plane separated by a low-loss dielectric material. A cross-sectional view as well as the quasi-TEM mode pattern[5] is shown in Fig. 5–11. Since the top surface is easily accessible, it is very convenient to mount

[5] Strictly speaking, the mode is not transverse electromagnetic. The fact that the insulating region consists of two different materials (air and the dielectric) requires the presence of longitudinal field components.

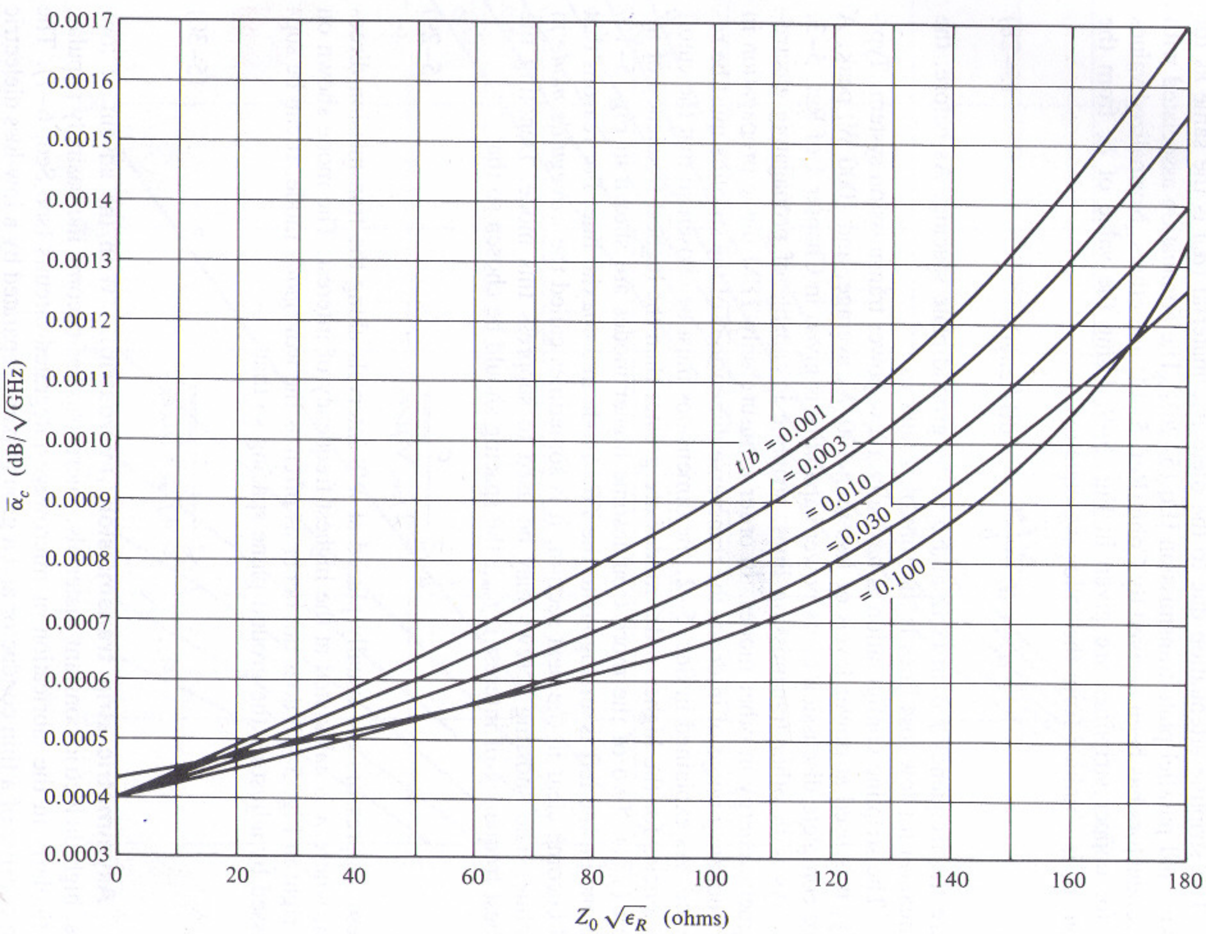


**Figure 5–9** Theoretical attenuation (normalized) of copper shielded stripline. Equation (5-28) is used to calculate $\alpha_c$. (From S. Cohn, Ref. 5–14; © 1955 IRE now IEEE, with permission.)

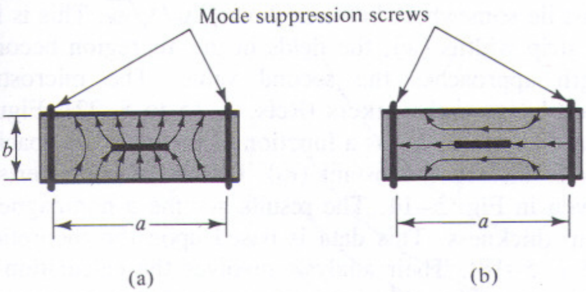


**Figure 5–10** Electric field patterns for two higher-order stripline modes.

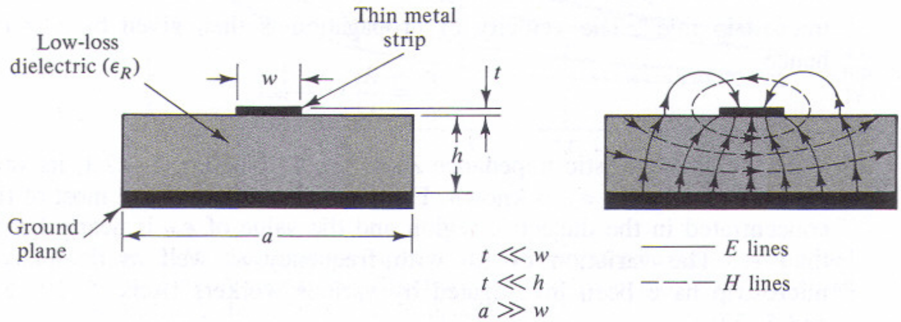


**Figure 5–11** An asymmetric strip transmission line (microstrip) and its quasi-TEM field pattern (cross-sectional view).

discrete devices and make minor adjustments in the microstrip circuit. Three commonly used dielectric materials are alumina, quartz, and Duroid®. The microwave properties of the first two are listed in Appendix B. Duroid is a registered trademark of the Rogers Corporation, Rogers, Connecticut.

Microstrip circuits and components are fabricated using printed circuit techniques. When semiconductor devices are to be integrated into the microstrip structure, silicon ($\epsilon_R = 11.8$) is often used as the dielectric. The use of high $\epsilon_R$ materials reduces the amount of fringing fields in the air region above the conductor. In most cases, the fields are negligible at a distance $2h$ above the metal conductor. To prevent radiation losses, the complete microstrip circuit is usually placed in a metal enclosure as shown in Fig. 5–12.

Since the insulating region in microstrip consists of more than one dielectric, Eqs. (2–53) and (2–55) *cannot* be used to calculate propagation velocity and wavelength. With fields in both the air and dielectric regions, one might suspect that the

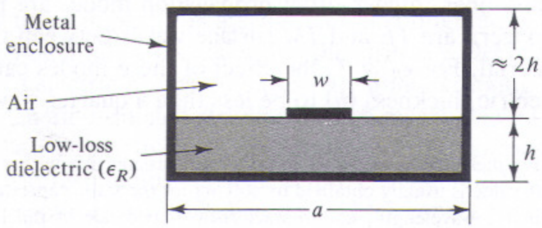


**Figure 5–12** An enclosed microstrip configuration used to prevent radiation losses.

actual value of wavelength must lie somewhere between $\lambda_0$ and $\lambda_0/\sqrt{\epsilon_R}$. This is indeed the case. For very wide strip widths ($w$), the fields in the air region become negligible and the wavelength approaches the second value. The microstrip configuration has been analyzed by several workers (Refs. 5–15 to 5–22). Figure 5–13 shows the normalized wavelength ($\lambda/\lambda_0$) as a function of the width-to-spacing ratio ($w/h$) for several values of dielectric constant ($\epsilon_R$). Curves of characteristic impedance versus $w/h$ are given in Fig. 5–14. The results assume a nonmagnetic dielectric and a negligible strip thickness. This data is based upon the theoretical work of Bryant and Weiss (Ref. 5–18). Their analysis involves the calculation of capacitance per length for the microstrip *with* and *without* the dielectric present. The ratio of capacitances is defined as the effective dielectric constant ($\epsilon_{\text{eff}}$) of the microstrip line.[6] The velocity of propagation is then given by $v = c/\sqrt{\epsilon_{\text{eff}}}$ and hence

$$\frac{v}{c} = \frac{\lambda}{\lambda_0} = \frac{1}{\sqrt{\epsilon_{\text{eff}}}} \tag{5–31}$$

With the characteristic impedance $Z_0 = 1/v\,C'$ [see Eq.(5–27)], its value can also be determined once $\epsilon_{\text{eff}}$ is known. For the higher values of $\epsilon_R$, most of the energy is concentrated in the dielectric region and the value of $\epsilon_{\text{eff}}$ is nearly but slightly less than $\epsilon_R$. The variation of $\epsilon_{\text{eff}}$ with frequency as well as dissipative losses in microstrip have been investigated by various workers (Refs. 5–19, 5–20, 5–21, and 5–22).

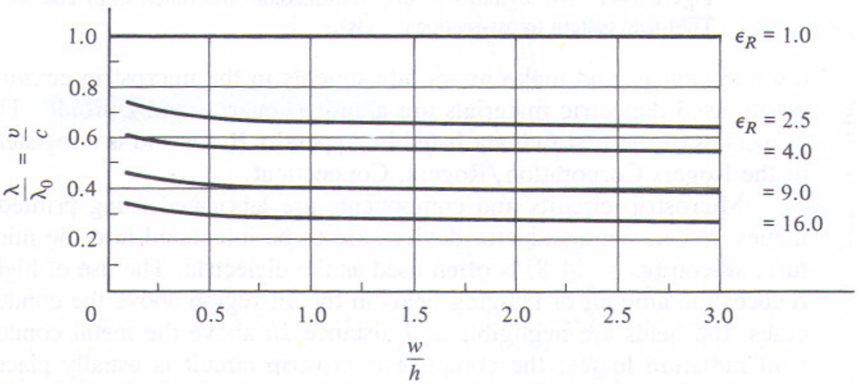


**Figure 5–13** Velocity and wavelength for TEM microstrip transmission. A nonmagnetic dielectric is assumed ($\mu_R = 1.0$). (From Bryant and Weiss, Ref. 5–18; © 1968 IEEE, with permission.)

As with all transmission lines, higher-order propagation modes are possible in microstrip. Of particular concern are *TE* and *TM* surface waves between the ground plane and the dielectric material. For $\epsilon_R \gg 1$, the effect of these modes can be minimized by choosing the dielectric thickness ($h$) to be less than a quarter wavelength at

[6] The concept of an effective dielectric constant ($\epsilon_{\text{eff}}$) for a transmission line with a nonuniform insulating region is very useful. Its value is usually obtained by solving for the static capacitance per unit length of the structure. The velocity, wavelength, and characteristic impedance of the line are then determined by assuming a *uniform* dielectric region of value $\epsilon_{\text{eff}}$ [Eqs. (5–31) and (5–27)].

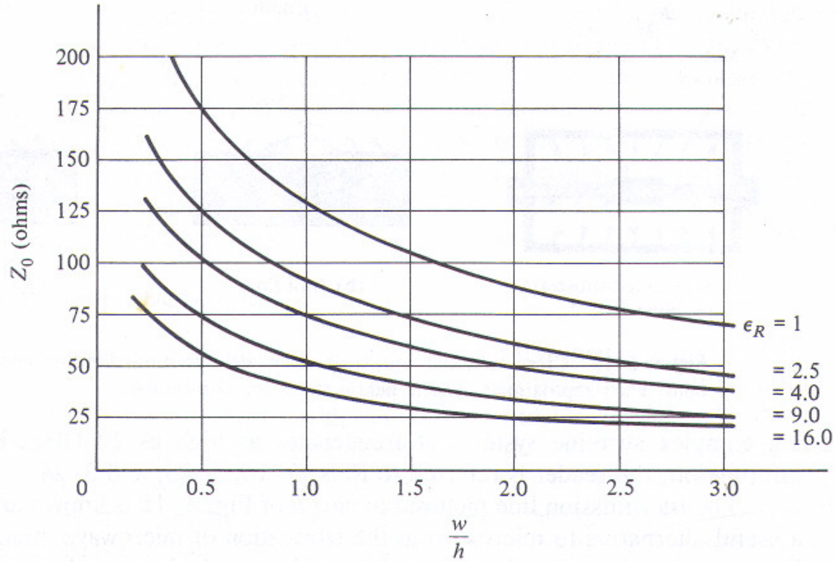


**Figure 5–14** Characteristic impedance for the microstrip configuration described in Fig. 5–11. A nonmagnetic dielectric is assumed ($\mu_R = 1.0$). (From Bryant and Weiss, Ref. 5–18; © 1968 IEEE, with permission.)

the highest frequency of interest ($f_{\max}$). Assuming a nonmagnetic dielectric, this requires

$$h < \frac{c}{4 f_{\max}\sqrt{\epsilon_r}} \tag{5–32}$$

A TE mode similar to the one in stripline (Fig. 5–10a) can also be troublesome. To minimize its effect, the strip width ($w$) should be restricted so that

$$w < \frac{c}{2 f_{\max}\sqrt{\epsilon_R}} \tag{5–33}$$

The above inequalities are approximate. More exact guidelines may be found in the literature.

**Other strip transmission lines.** Figure 5–15 shows three additional transmission-line systems that utilize printed-circuit technologies. Their approximate TEM electric field patterns are also shown. The suspended-substrate stripline pictured in part $a$ is a symmetrical configuration because the two strips are at the same potential. Consequently, the primary electric field is in the air region, while the dielectric region contains only minor fringing fields. Thus the structure is essentially an air-insulated stripline, which means that its dielectric loss ($\alpha_d$) is negligible. Since $\epsilon_{\text{eff}}$ is practically unity, transverse dimensions and wavelength are larger than in a corresponding dielectric-filled stripline. This is an advantage in high-frequency applications since dimensional tolerances become less stringent. As a result, the suspended-substrate technique provides an accurate and economical method for fabricat-

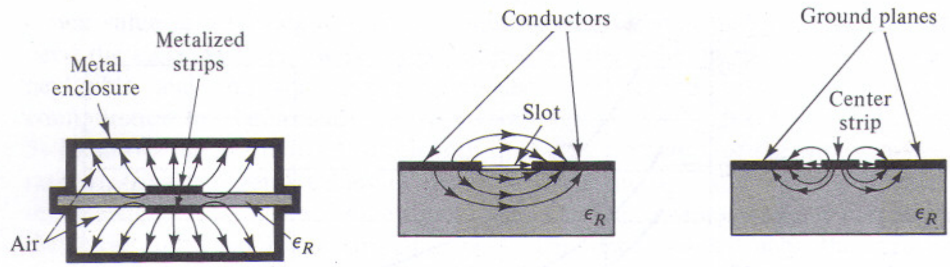


(a) Suspended-substrate stripline (b) Slot line (c) Coplanar line

**Figure 5–15** Cross-sectional views of other strip transmission-line configurations. Their approximate electric field patterns are also shown.

ing complex stripline systems at frequencies as high as 20 GHz. For additional information, the reader is referred to Refs. 5–16, 5–23, and 5–24.

The transmission line pictured in part *b* of Fig. 5–15 is known as *slot line*. It is a useful alternative to microstrip in the fabrication of microwave integrated circuits. For example, since the electric field is as shown, devices can be easily shunt connected to the line. Microstrip, on the other hand, lends itself to series-connected devices. Also, high values of $Z_0$ are easily realized in slot line, while low values are more easily achieved with microstrip. In slot line, the magnetic field (not shown) has a strong component in the propagation direction. Therefore, the primary transmission mode is *not* TEM but TE. This characteristic is useful when the system requires the incorporation of nonreciprocal ferrite components. The slot line has been analyzed by Cohn (Ref. 5–25) and others (Refs. 5–26 and 5–27). These articles provide detailed design information on velocity, wavelength, and impedance.

The coplanar line, shown in part *c* of the figure, consists of a thin metal strip with ground planes on either side. Also shown is the approximate electric field pattern. This structure has been analyzed by Wen (Ref. 5–28) and Davis (Ref. 5–29). It combines some of the advantages of microstrip and slot lines. For example, both series and shunt connections are easily achieved in coplanar line. Also, since a significant longitudinal magnetic field component is present, nonreciprocal ferrite components can be realized.

An excellent comparison of microstrip, slot line, and coplanar line is found in Ref. 5–7. A wealth of design data is also included.

## 5-4 RECTANGULAR AND CIRCULAR WAVEGUIDES

Hollow waveguides are commonly used as transmission lines at frequencies above 5 GHz. Compared to coaxial transmission, waveguides have the following advantages.

1. Higher power handling capability.
2. Lower loss per unit length.
3. A simpler, lower cost mechanical structure.

In addition, the reflections caused by the flanges used in connecting waveguide sections is usually less than that associated with coaxial connectors. The disadvantages of waveguide transmission are larger cross-sectional dimensions and a lower usable bandwidth than coaxial transmission. The fact that hollow waveguides can support electromagnetic waves is proven mathematically in Sec. 5–5. The properties of these waves are described in detail and appropriate equations are derived. In this section, the explanation is given in terms of TEM waves and the transmission-line concepts developed in Chapter 3.

### 5–4a Rectangular Waveguide

Figure 5–16 shows a rectangular waveguide of inner dimensions $a$ and $b$. This represents the most common configuration for waveguide transmission. It is customary to label the broad dimension or guide width as $a$ and the height as $b$. Typically, the conducting walls are made of brass or aluminum and the dielectric region is usually air. The following discussion shows that under certain conditions, electromagnetic waves can propagate along the inside of the waveguide. It is assumed that the wall thickness is greater than several skin depths and hence does not enter into the analysis.

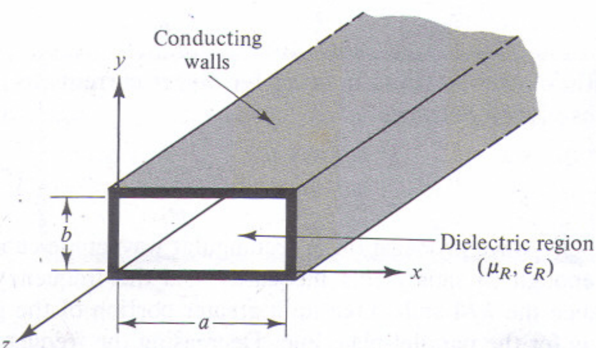


**Figure 5–16** The rectangular waveguide structure.

Figure 5–17 shows a parallel-plate transmission line similar to that in Fig. 5–6. The width of the metal strips is $w$ and their spacing is $b$. The $E$ and $H$ field patterns are also shown. Power is delivered to the load via longitudinal current flow along the two strips. Suppose now that a pair of shorted stubs of length $l$ are connected to the parallel-plate line as shown. If the stubs are a quarter wavelength long, they will have no effect on the transmission of power since they present an infinite impedance in shunt with the line. The $E$ and $H$ standing wave patterns for the shorted stubs are also shown in the figure. The current flow in the stubs is reactive since no real power can be delivered to the shorts. The longitudinal current, on the other hand, can deliver power and hence is referred to as the *power* current. Note that the direction of the *reactive* and *power* currents are perpendicular to each other. One can imagine an infinite set of these quarter wavelength shorted stubs connected in shunt with the parallel-plate line. The resultant configuration is exactly the rectangular waveguide shown in Fig. 5–16 where

$$a = 2l + w$$